

# Light harvesting of silicon nanostructure for solar cells application

Yingfeng Li,<sup>1</sup> Luo Yue,<sup>2</sup> Younan Luo,<sup>1</sup> Wenjian Liu,<sup>1</sup> and Meicheng Li<sup>1,3,\*</sup>

<sup>1</sup>State Key Laboratory of Alternate Electrical Power System with Renewable Energy Sources, North China Electric Power University, Beijing, 102206, China

<sup>2</sup>College of Science and State Key Laboratory for Heavy Oil Processing, China University of Petroleum, Beijing 102249, China

<sup>3</sup>Chongqing Materials Research Institute, Chongqing, 400707, China

\*mcli@ncepu.edu.cn

**Abstract:** Silicon nanostructures have light-harvesting effects for enhancing the performance of solar cells. Based on theoretical investigations on the optical properties of silicon nanowire (Si NW), the influencing laws of the size of Si NW on its light-harvesting effect are proposed. For the first time, we reveal that the resonant wavelength of Si NW predicted by the leaky mode theory does not correspond to the actual resonant wavelength calculated by the discrete dipole approximation method, but exactly coincides with the leftmost wavelength of the resonance peak. Then, the size dependency of the resonant intensity and width of Si NW is different from that of spherical nanoparticles, which can be deduced from the Mie theory. The size dependencies of resonant intensity and width are also applicative for silver/silicon composite nanowires. In addition, it is found that the harvested light by the Si and Ag/Si NW both show significant radial locality feature. The insight in this work is fundamental for the design and fabrication of efficient light - harvesting nanostructures for photovoltaic devices.

©2016 Optical Society of America

**OCIS codes:** (160.4760) Optical properties; (290.4020) Mie theory; (290.5825) Scattering theory.

---

## References and links

1. C. Xie, B. Nie, L. Zeng, F.-X. Liang, M.-Z. Wang, L. Luo, M. Feng, Y. Yu, C.-Y. Wu, Y. Wu, and S. H. Yu, "Core-Shell Heterojunction of Silicon Nanowire Arrays and Carbon Quantum Dots for Photovoltaic Devices and Self-Driven Photodetectors," *ACS Nano* **8**(4), 4015–4022 (2014).
2. G.-L. Zang, G.-P. Sheng, C. Shi, Y.-K. Wang, W.-W. Li, and H.-Q. Yu, "A bio-photoelectrochemical cell with a MoS<sub>2</sub>-modified silicon nanowire photocathode for hydrogen and electricity production," *Energy Environ. Sci.* **7**(9), 3033–3039 (2014).
3. T. Song, S.-T. Lee, and B. Sun, "Silicon nanowires for photovoltaic applications: The progress and challenge," *Nano Energy* **1**(5), 654–673 (2012).
4. B. Tian, X. Zheng, T. J. Kempa, Y. Fang, N. Yu, G. Yu, J. Huang, and C. M. Lieber, "Coaxial silicon nanowires as solar cells and nanoelectronic power sources," *Nature* **449**(7164), 885–889 (2007).
5. H. Park and K. B. Crozier, "Elliptical silicon nanowire photodetectors for polarization-resolved imaging," *Opt. Express* **23**(6), 7209–7216 (2015).
6. J. K. Mann, R. Kurstjens, G. Pourtois, M. Gilbert, F. Dross, and J. Poortmans, "Opportunities in nanometer sized Si wires for PV applications," *Prog. Mater. Sci.* **58**(8), 1361–1387 (2013).
7. K.-Q. Peng, X. Wang, L. Li, Y. Hu, and S.-T. Lee, "Silicon nanowires for advanced energy conversion and storage," *Nano Today* **8**(1), 75–97 (2013).
8. M. D. Kelzenberg, S. W. Boettcher, J. A. Petykiewicz, D. B. Turner-Evans, M. C. Putnam, E. L. Warren, J. M. Spurgeon, R. M. Briggs, N. S. Lewis, and H. A. Atwater, "Enhanced absorption and carrier collection in Si wire arrays for photovoltaic applications," *Nat. Mater.* **9**(3), 239–244 (2010).
9. Y. Li, M. Li, D. Song, H. Liu, B. Jiang, F. Bai, and L. Chu, "Broadband light-concentration with near-surface distribution by silver capped silicon nanowire for high-performance solar cells," *Nano Energy* **11**, 756–764 (2015).
10. Y. Li, M. Li, R. Li, P. Fu, B. Jiang, D. Song, C. Shen, Y. Zhao, and R. Huang, "Linear length-dependent light-harvesting ability of silicon nanowire," *Opt. Commun.* **355**, 6–9 (2015).

11. Y. Li, M. Li, R. Li, P. Fu, L. Chu, and D. Song, "Method to determine the optimal silicon nanowire length for photovoltaic devices," *Appl. Phys. Lett.* **106**(9), 091908 (2015).
12. Y. Li, M. Li, P. Fu, R. Li, D. Song, C. Shen, and Y. Zhao, "A comparison of light-harvesting performance of silicon nanocones and nanowires for radial-junction solar cells," *Sci. Rep.* **5**, 11532 (2015).
13. H. Bao, W. Zhang, L. Chen, H. Huang, C. Yang, and X. Ruan, "An investigation of the optical properties of disordered silicon nanowire mats," *J. Appl. Phys.* **112**(12), 124301 (2012).
14. E. Garnett and P. Yang, "Light trapping in silicon nanowire solar cells," *Nano Lett.* **10**(3), 1082–1087 (2010).
15. L. Cao, P. Fan, A. P. Vasudev, J. S. White, Z. Yu, W. Cai, J. A. Schuller, S. Fan, and M. L. Brongersma, "Semiconductor nanowire optical antenna solar absorbers," *Nano Lett.* **10**(2), 439–445 (2010).
16. L. Cao, J. S. White, J.-S. Park, J. A. Schuller, B. M. Clemens, and M. L. Brongersma, "Engineering light absorption in semiconductor nanowire devices," *Nat. Mater.* **8**(8), 643–647 (2009).
17. T. Coenen, J. van de Groep, and A. Polman, "Resonant modes of single silicon nanocavities excited by electron irradiation," *ACS Nano* **7**(2), 1689–1698 (2013).
18. B. Luk'yanchuk, N. I. Zheludev, S. A. Maier, N. J. Halas, P. Nordlander, H. Giessen, and C. T. Chong, "The Fano resonance in plasmonic nanostructures and metamaterials," *Nat. Mater.* **9**(9), 707–715 (2010).
19. L. Yu, S. Misra, J. Wang, S. Qian, M. Foldyna, J. Xu, Y. Shi, E. Johnson, and P. R. I. Cabarcas, "Understanding Light Harvesting in Radial Junction Amorphous Silicon Thin Film Solar Cells," *Sci. Rep.* **4**, 1–7 (2014).
20. J. A. Schuller, E. S. Barnard, W. Cai, Y. C. Jun, J. S. White, and M. L. Brongersma, "Plasmonics for extreme light concentration and manipulation," *Nat. Mater.* **9**(3), 193–204 (2010).
21. H. A. Atwater and A. Polman, "Plasmonics for improved photovoltaic devices," *Nat. Mater.* **9**(3), 205–213 (2010).
22. B. T. Draine and P. J. Flatau, "Discrete-dipole approximation for scattering calculations," *J. Opt. Soc. Am. A* **11**(4), 1491–1499 (1994).
23. P. J. Flatau and B. T. Draine, "Fast near field calculations in the discrete dipole approximation for regular rectilinear grids," *Opt. Express* **20**(2), 1247–1252 (2012).
24. B. T. Draine and P. J. Flatau, "User guide for the discrete dipole approximation code DDSCAT 7.3," arXiv:1305.6497 (2013).
25. J. van de Groep and A. Polman, "Designing dielectric resonators on substrates: Combining magnetic and electric resonances," *Opt. Express* **21**(22), 26285–26302 (2013).
26. B. Hua, B. Wang, M. Yu, P. W. Leu, and Z. Fan, "Rational geometrical design of multi-diameter nanopillars for efficient light harvesting," *Nano Energy* **2**(5), 951–957 (2013).
27. D. W. Lynch and W. Hunter, Comments on the optical constants of metals and an introduction to the data for several metals, *Handbook of Optical Constants of Solids* (Academic Press, 1985).
28. J. Geist, The index of refraction of silicon in the visible and very near IR-Silicon (Si) Revisited (1.1–3.1 eV), *Handbook of Optical Constants of Solids* (Academic Press, 1998).
29. Y. Yu and L. Cao, "Coupled leaky mode theory for light absorption in 2D, 1D, and 0D semiconductor nanostructures," *Opt. Express* **20**(13), 13847–13856 (2012).

## 1. Introduction

Recent years, silicon nanowire (Si NW) has been found to have strong light-harvesting effect. And due to the great application potential of it in photovoltaic devices [1–6], considerable theoretical and experimental investigations [7–16] have been carried out on its optical properties. These investigations denote that Si NW has several unique features in light-harvesting. At First, Si NW had excellent light-harvesting multiples. It can capture light in an area more than 100 times of its geometrical cross section [7]. Secondly, the resonance wavelengths of Si NW generally range from 400 to 700 nm [17], which just locates at the spectrum range corresponding to the high irradiance of *AMI.5*. Thirdly, due to the dielectric nature of silicon material, the optical losses coming from the parasitic absorption, like in metallic resonant nanostructures, can be absolutely avoided in Si NW. Fourthly, the distribution of the harvested light by Si NW is manipulatable by adjusting its diameter or shape. This is because the light-harvesting ability of Si NW comes from the Fano resonances [18], thus most of the harvested light will be confined within the nanowire and propagate in waveguide modes. The mode distribution within the nanowire is adjustable and naturally inhomogeneous in radial direction [19]. These features indicate that Si NW is particularly suitable for light-harvesting applications in solar cells, which is even more effective than the fashionable plasmonic light-harvesting strategy [20, 21].

In this work, based on our recent theoretical works on the optical properties of Si NW, we first gave the clear light-harvesting mechanism of it, and summarized the influencing laws of

its size on the light-harvesting effect. Then, discrete dipole approximation (DDA) [22–24] simulations are carried out for a series of silver/silicon composite nanowires (Ag/Si NWs), which have constant total length. It is found that the light-harvesting effects of the Ag and Si parts are nearly non-interfering, which follow the same laws as an individual Si NW. Finally, radius locality feature of the harvested light within and out the nanowire is analyzed. These works provide fundamental insights for the using of Si NW as building blocks in photovoltaic devices.

## 2. Model and method

The Si NW and Ag/Si NW are both modeled as circular cylinder with hemisphere tip, as shown in Fig. 1(a) and 1(b). The light-harvesting effects of them can be characterized by the extinction and absorption efficiencies, see Figs. 1(c) and 1(d). The lengths and diameters of Si NWs are varied, which range from 0.2 $\mu\text{m}$  to 10 $\mu\text{m}$  and from 40nm to 150nm, respectively. The total length of the Ag/Si NWs (including the rounded cap) is set to 3 $\mu\text{m}$ , and the length of the silver part (including the cap) changes from 0 $\mu\text{m}$  to 3 $\mu\text{m}$  gradually. The extinction and absorption efficiencies are calculated by the DDA method, whose framework can be found elsewhere. Here, we just give the key settings used, and the physical significances of the quantities, extinction and absorption efficiency.

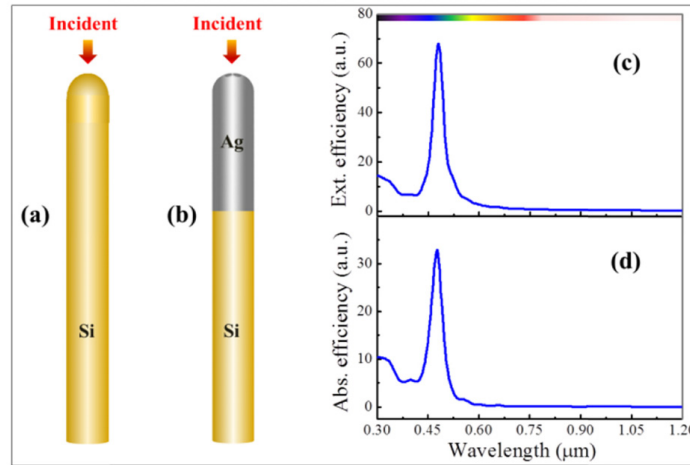


Fig. 1. Model of the (a) Si NW and (b) Si/Ag NW; and the (c) extinction and (d) absorption efficiencies of a Si NW (diameter 70nm and length 0.5 $\mu\text{m}$ ).

The extinction and absorption efficiencies are defined as  $Q_{ext} = C_{ext}/\pi r^2$  and  $Q_{abs} = C_{abs}/\pi r^2$ , where  $C_{ext}$ ,  $C_{abs}$ , and  $\pi r^2$  denote the extinction, absorption and real geometric cross section of the NW. They reflect the light concentration (extinction) and light absorption abilities of the NWs, respectively. The calculation accuracy of DDA depends on two factors: the interdipole spacing ( $d$ ) and the error tolerance between two adjacent iterative steps ( $h$ ). These two parameters have been carefully tested [9, 11], and are set to 3.3nm and  $1.0 \times 10^{-5}$  respectively. Due to the polarization-independency [16, 25] for the light-absorption ability of Si NW, only incident linearly polarized light is considered. And since for the solar cells application of Si NW the incident angle is usually small, meanwhile the light-absorption ability of Si NW is weak angle-dependent [15, 26], only illumination from the tip (corresponds to incident angle  $\theta = 0^\circ$ ) is taken into account. Bulk values of the complex index of refraction for silver and silicon [27, 28] are used.

### 3. Results and discussion

#### 3.1 Resonant wavelength of Si NW

The light-harvesting effect of Si NW comes from the coupling between the leaky modes and the light around it, thus is dramatically wavelength dependent. Therefore, resonant wavelength of the Si NW should be a very important characteristic quantity. According to the leaky mode theory [29], the resonant wavelength can be predicted by calculating the cut-off wavelength of mode supported by the NW. For the lowest order resonant, the cut-off wavelength can be calculated by letting the normalized frequency  $V$  equal to its cut-off parameters, 2.405.  $V = \pi d / \lambda \sqrt{n^2 - 1}$ , where  $d$  is the Si NW diameter,  $n$  is the refractive index of silicon, and  $\lambda$  is the wavelength of light. From this equation it can be seen clearly that the resonant wavelength is only diameter dependent and nearly linearly with the diameter.

This dependence can be perfectly reflected by our calculated results on the extinction efficiency of Si NWs with fixed length (1 $\mu\text{m}$ ) and various diameters, as given in the inset of Fig. 2(a). The resonant wavelengths for Si NWs with diameters 40, 60, 80, 100, 120 and 140 nm are 410, 454, 520, 600, 683 and 768nm, respectively. However, these values not exactly equal to but some greater than those predicted by the above equation, 370, 410, 460, 530, 600 and 680nm. This makes clear that the actual resonant wavelengths are not the cut-off wavelengths. From the black spheres in Fig. 2(a) we can see that, the calculated cut-off wavelengths exactly correspond to the leftmost wavelengths of the resonance peaks. This denotes the cut-off wavelength is just a critical wavelength where the mode can be leaked out, and at this wavelength, only very little light can be leaked out and couple with the light surrounding the NW. With wavelength increases, more light can be leaked out, and correspondingly more light can be coupled within the Si NW, till the actual resonant wavelength. However, when the wavelength is much longer than the cut-off wavelength, the leaky mode cannot be supported again thus the resonant peak vanishes gradually.

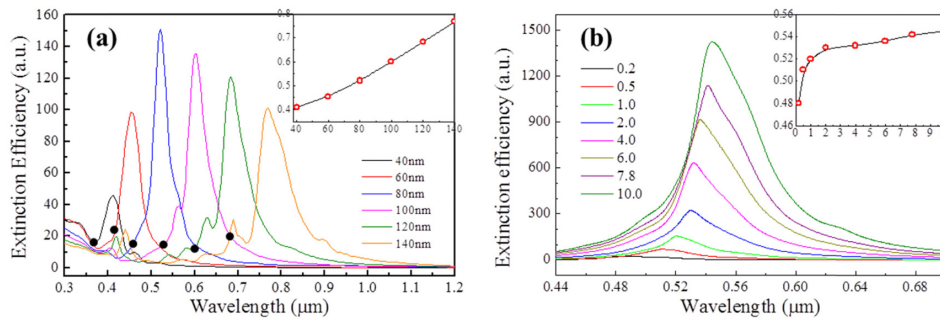


Fig. 2. (a) Diameter and (b) length dependency of the resonant wavelength of Si NW.

The leaky mode theory is based on the precondition that the length of the nanowire is infinite; so it cannot be used to evaluate the length dependency of the resonant wavelength. We have calculated the extinction curves for Si NWs of fixed diameter, 80nm, and various lengths from 0.2 to 10 $\mu\text{m}$ , as given in Fig. 2(b); and given the length dependency of the resonant wavelengths in its inset. It can be obviously observed that, when the length is quite small, the resonant wavelength is also dramatically length dependent. While, with the length of Si NW increases, this dependency becomes weaker and weaker till can be neglected. The reason for this length dependency is that, in short Si NW, the light is not only 2D limited but 3D limited. If has no specific requirement on precision, the leaky mode theory can also be used to predict the resonant wavelength of Si NW with length greater than 1 $\mu\text{m}$ .

### 3.2 Intensity and width of the resonance peak with various Si NW sizes

The intensity of the resonance peak denotes the maximum light-harvesting multiples of Si NW; and the width of the resonance peak, which is characterized by the full width at half maximum here, reflects the actuating range of Si NW. They are both critical features for the light-harvesting ability of Si NW.

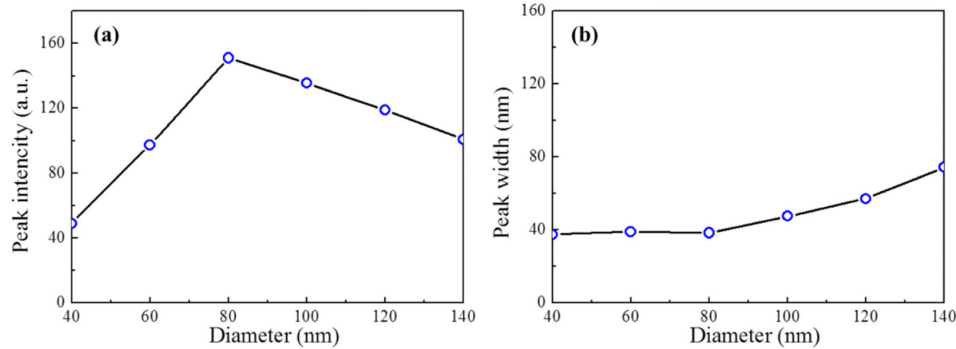


Fig. 3. Diameter dependency of the (a) intensity and (b) width of the resonance peak for the extinction efficiencies of Si NW.

Diameter dependencies of the peak intensity and width are investigated firstly. What are plotted in Fig. 3(a) are the peak intensities, which are extracted from the extinction curves in Fig. 2(a), versus the diameters of Si NW. Obviously, the peak intensities increase in linearity first, arrive at a turning point, and then decrease linearly. This changing tendency indicates that the Si NW should have an optimal diameter for light-harvesting, which is about 80nm. The underlying reasons for the appearance of the turning points in Fig. 3(a) and 3(b) are still not clear. From Fig. 2(a) it can be observed that, if the diameter of Si NW greater than 80nm, one high-order peak appears. We think the appearance of such high-order peak may be the main reason for the occurrence of the turning point. Before the turning point, the peak intensities increase with diameter, and their widths are nearly constant. While after the turning point, the peak intensities decreases with diameter, and the peak widths change to be increased with diameter.

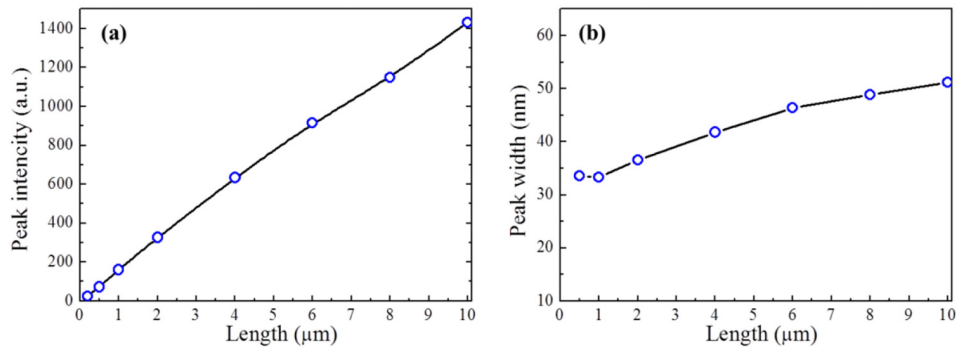


Fig. 4. Length dependency of the (a) intensity and (b) width of the resonance peak for the extinction efficiencies of Si NW.

Then, we investigate the length dependencies of the peak intensity and width. Figure 4 presents the relationships between the peak intensities, widths and the length of Si NW, draw from Fig. 2(b). On a brighter note, the extinction efficiencies at the resonant wavelength exhibit nearly perfect linear relationships with the Si NW length. Meanwhile, the widths of the resonance peaks also increase approximately linearly with the Si NW length.

Taking the linear dependencies of the peak intensity on the diameter and length into account together, it can be deduced that the extinction efficiency of Si NW is proportional to the area of its longitudinal section. According to the definition of the extinction efficiency above, this means the extinction cross section is proportional to *the product of the volume and diameter* of Si NW. This relationship is different from that of the spherical nanoparticles, which can be deduced by the Mie theory, where the extinction cross section is proportional to the volume of the target. For spherical nanoparticles, the maximum extinction cross-section  $\sigma_{\max}$  equals to  $\frac{2\pi\hbar\omega_0^2 r^3}{\Gamma c}$ , where  $\omega_0$  is the vacuum frequency of light,  $c$  is the speed of light,  $\Gamma = \hbar\omega_0\varepsilon''/6$  is the width of the resonance peak, and  $\varepsilon''$  is the imaginary part of dielectric constant.

Taking into account the diameter (considering the ones smaller than 80nm only) and length dependency of the peak width together, the peak width is only length dependent: it increases approximately linearly with the length of Si NW. This is also different from that for spherical nanoparticles,  $\Gamma = \hbar\omega_0\varepsilon''/6$ , where the resonant width is independent on the particle size. The deep physical reasons for such differences also need further studies.

### 3.3 The light-harvesting properties of Ag/Si NW

We have also investigated the extinction properties of a series of Ag/Si NWs with fixed diameter 80nm, fixed total length 3 $\mu\text{m}$ , but various length of the Ag part from 0 to 3 $\mu\text{m}$ . The obtained extinction curves are given in Fig. 5(a). It can be seen that, the resonant wavelengths of the Ag and the Si part both show the similar length dependency as the pure Si NW analyzed above.

The size dependencies of the peak intensity and width for Si NW mentioned above can also be reproduced for the Ag/Si NW. From Fig. 5(b) and 5(d), we can found that the peak intensities for the Ag and Si part are both linear to their respective lengths but not the total length. And From Fig. 5(d) and 5(e) it can be observed that the peak widths of the Ag and Si part also changes approximately linearly with their respective lengths. On the other hand, these results also indicate that, the light-harvesting properties of both the metal and semiconductor nanowires have the same size dependencies.

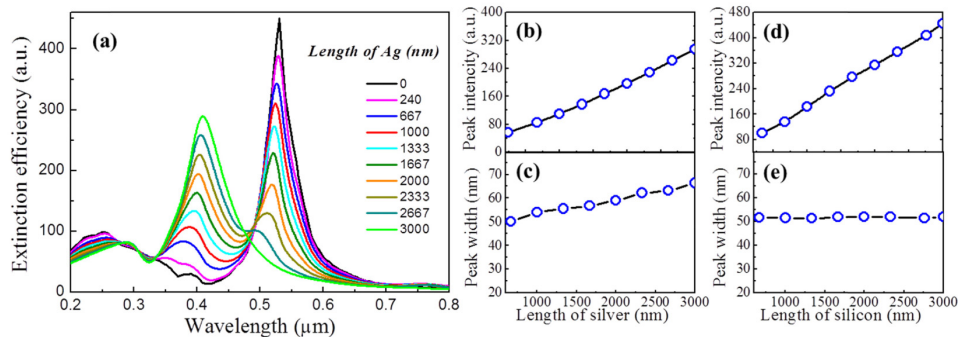


Fig. 5. (a) Extinction curves for the Ag/Si NWs; and the length dependency of the (b) intensity of the resonance peaks of Ag, (c) intensity of the resonance peaks of Si, (d) width of the resonance peaks of Ag, and (e) width of the resonance peaks of Si.

### 3.4 Radius locality of the harvested light

Besides the regularity found above, we have also investigated the spatial distributions of the light harvested by the Si and Ag/Si NW. It is found that the light harvested by the Si and Ag/Si NW shows notable radial locality feature. From Fig. 6(a), the angle distribution curves of the scattered light by a Si NW with 80nm diameter and 2.3 $\mu\text{m}$  length, it can be seen that

most of the scattered light distributes in a narrow angle range  $\theta < 20^\circ$ . In quantitative terms, the forward scattering fraction can reach about 99.8%.

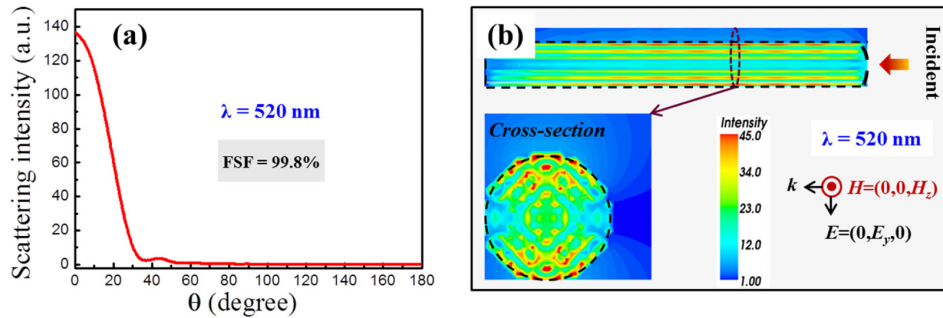


Fig. 6. (a) Angular distribution for the scattered light without the SiNW, and (b) spatial distributions for the absorbed light within the Si NW.

Figure 6(b) shows the spatial distributions for the light confined within a Si NW of 80nm diameter and  $0.5\mu\text{m}$  length. Clearly, the distribution maps also show radial locality feature since they are determined by the waveguide modes supported by the nanowire. We have calculated the spatial distributions of the light within the silicon part of the Ag/Si NW quantitatively. It has been found that [9] over 95% of the light collected by the plasmonic effect of Ag and over 91% of the light coupled by the Fano resonance of Si will distribute within a thin surface layer of the nanowire with thickness 20nm, respectively.

As a summary, both the harvested lights within and around the nanowire show obviously radial locality feature. Most of them will distribute at the region near the surface of the nanowire, which just corresponds to the junction region in radial junction Si NW based solar cells. So, Si and Ag/Si NW are both very suitable to be used in fabricating radial junction photovoltaic devices.

#### 4. Conclusion

Based on DDA calculations on the optical properties of Si and Ag/Si NWs, we have given a clear physical image for the light-harvesting mechanism of nanowire structures, and found out the laws for how the size influences the light-harvesting effect. The light-harvesting effect of Si NW comes from coupling the surround light into the leaky modes it supported; therefore, the resonant wavelength of Si NW depends dramatically on its diameter. However, we found that the resonant wavelengths predicted by the leaky mode theory are not precisely equal to the ones obtained using DDA calculations, but exactly correspond to the leftmost ones of resonance peaks. Before the appearance of high-order resonances (diameter smaller than 80nm), the resonant intensity of Si NW increases both proportionally to diameter and length. This means the extinction cross section of Si NW is proportional to the product of its volume and diameter, which is different from the relationships deduced from the Mie theory, where the extinction cross section is only proportional to the volume of the target. We also found that the resonant width of Si NW is approximately linear to its length, which is different from that deduced by the Mie theory too, where resonant width shows no dependence on the size of target. These regularities are also applicable for the Ag/Si NW, or more strictly speaking, for the Ag part and the Si part in the Ag/Si NW. The peak intensities of the Ag and Si part, and the peak widths of them, are both linear to their respective lengths. In addition, no matter the lights scattered and absorbed by the Si and Ag/Si NW show significant radius locality feature, which indicates that the nanowire structure is quite suitable to be used in fabrication radial-junction solar cells. This work is great helpful for the future design and development of more efficient light-harvesting silicon nanostructures in photovoltaic applications.

## **Acknowledgments**

This work is supported partially by National High-tech R&D Program of China (863 Program, No. 2015AA034601), National Natural Science Foundation of China (Grant nos. 91333122, 51402106, 51372082, 61204064 and 51202067), Ph.D. Programs Foundation of Ministry of Education of China (Grant nos. 20130036110012), Par-Eu Scholars Program, and the Fundamental Research Funds for the Central Universities.